

COMPONENTS OF LASER SYSTEMS

PACS numbers: 42.79.Ci; 42.25.Ja; 42.70.Ce
DOI: 10.1070/QE2009v039n01ABEH013876

Characteristics of Cornu depolarisers made from quartz and paratellurite optically active crystals

V.A. Bagan, B.L. Davydov, I.E. Samartsev

Abstract. **Cornu depolarisers made from quartz and paratellurite crystals have been studied. Numerical calculations and experimental data demonstrate that such depolarisers make it possible to significantly alleviate the major drawback to birefringent wedge depolarisers: the strong dependence of the polarisation of the output beam on the input polarisation orientation. We have examined the polarisation extinction ratio in the depolarisers as a function of the rotatory power of the crystals, depolariser length, beam diameter, and power distribution across the beam, and have determined the angle between the circularly polarised output beams in the far field. Data on the optical rotatory power of quartz and paratellurite crystals have been systematized, and the results have been used to derive dispersion formulas for these materials in the visible and near-IR spectral regions.**

Keywords: *Cornu depolariser, optical activity of quartz, paratellurite*.

1. Introduction

Among components of laser systems are laser radiation depolarisers, which 'intermix' polarisation states either in time (Billings depolariser [1]), or by spectral components (Lyot depolariser [2]) or by multiple zones in the cross section of the beam (spatial depolarisers [3]). In this paper, we present a study of spatial depolarisers consisting of optically contacted identical wedges made from optically active crystals, the so-called Cornu depolarises [3]. Such studies are of high current interest not only because there is little information about such depolarisers but also in the context of elimination of polarisation fading in the heterodyne receiver circuit of lidar systems, when the arbitrary polarised backscattered radiation interacts with the reference heterodyne signal to form an interference pattern in the active area of the photodetector.

V.A. Bagan, B.L. Davydov, I.E. Samartsev V.A. Kotel'nikov Institute of Radio Engineering and Electronics (Fryazino Branch), Russian Academy of Sciences, pl. Vvedenskogo 1, 141190 Fryazino, Moscow region, Russia; e-mail: bld_res2000@rambler.ru

Received 11 April 2008; revision received 22 May 2008
Kvantovaya Elektronika **39** (1) 73 – 78 (2009)
Translated by O.M. Tsarev

Currently, use is mainly made of a simple, relatively inexpensive depolariser consisting of a pair of thin wedges, one made of an optically anisotropic crystal (as a rule, quartz), and the other of glass [4]. In this design, the optical axis of the crystalline wedge is normal to the wave vector of the input beam, and the polarisation states in particular zones in the cross section of the beam depend on the relative phase shift between the ordinary and extraordinary waves. This wave plate principle assumes that the degree of depolarisation strongly depends on the polarisation state of the light. In particular, if the input beam is polarised in a plane parallel or normal to the optical axis of the crystal, no spatial depolarisation occurs. It is for this reason that wedge depolarisers are used mainly for spatial depolarisation of light beams whose polarisation plane is at $\pm 45^\circ$ to the optical axis of the crystal. In addition, a birefringent depolariser creates in the far field two non-parallel beams with orthogonal linear polarisations, whose intensities vary in antiphase from zero to maximum values at incoming beam polarisations arbitrary in time. It is easy to calculate that, for a depolariser consisting of two optically contacted or cemented wedges identical in geometry, one from single-crystal SiO_2 (ordinary and extraordinary refractive indices $n_o(1060\ \text{nm}) \approx 1.5341$ and $n_e(1060\ \text{nm}) \approx 1.5428$) and the other from BK-8 glass ($n(1060\ \text{nm}) \approx 1.536$), with a wedge angle from 10° to 45°, the angle between the output beams in air will be $5'$ to $30'$. This implies that spatial depolarisation will be effective only in that part of the near field where the separation between the beams is small.

The use of a more complicated depolariser design, e.g., consisting of two birefringent wedges with their optical axes 45° apart, might be expected to obviate the above problem because a third, central output beam appears in which the orthogonally polarised waves are parallel [5]. With this design, however, the output beam intensity will also vary from zero to a maximum value upon 'circular' variation of the polarisation direction of the input beam.

As distinct from birefringent depolarisers, the Cornu depolariser takes advantage of the optical activity of the crystals it consists of, which leads to rotation of the polarisation ellipse as the light passes through the optically active material. The ellipse rotation angle φ is determined by the phase retardations of left- and right-circularly polarised light, i.e. by the corresponding refractive indices n_L and n_R [6]:

$$\varphi = \rho L, \tag{1}$$

where $\rho = (\pi/\lambda_0)(n_L - n_R)$ is the optical rotatory power,

$n_L = n_o + \lambda_0\rho/(2\pi)$, $n_R = n_o - \lambda_0\rho/(2\pi)$, L is the crystal length and λ_0 is the wavelength of the light in vacuum.*

The Cornu depolariser also consists of two identical crystalline wedges.** The wedges should be cut from similar crystals (e.g. those of quartz) opposite in the direction of rotation and should be oriented so that the light propagation direction is parallel to their optical axis (Fig. 1). With this design, the angle of rotation φ varies across the beam. In contrast to birefringent depolarisers, this device is capable of depolarising the input beam at any orientation of its polarisation ellipse.

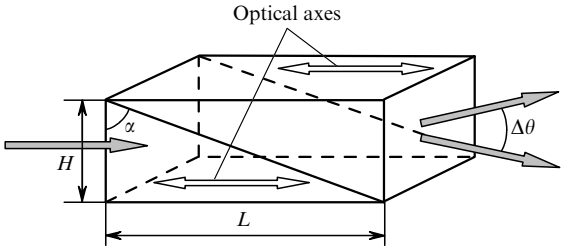

Figure 1. Cornu depolariser consisting of two wedges identical in chemical composition but opposite in the direction of optical rotation. The angle between the output beams, $\Delta\theta$, and their displacement are grossly exaggerated for clarity. The depolariser height was $H = 10$ mm in all experiments and calculations.

The far-field behaviour of the two output beams differs markedly from that outlined above. Since $n_L \neq n_R$, there is also some separation between the beams in the far field, but they are left- and right-circularly polarised rather than linearly polarised. Moreover, because of the small difference between n_L and n_R $\{\lambda_0\rho/(2\pi) \sim 10^{-5}$ to 10^{-4} in the IR spectral region [6]$\}$, the angle between the output beams must be substantially smaller even at large wedge angles α (Fig. 1), characteristic of this depolariser.

The objective of this work was to experimentally and theoretically study the basic characteristics of the Cornu depolariser, with particular attention to its performance at arbitrary polarisation states of the input radiation, to the optimisation of the material of the depolariser and its length and to the polarisation states of the output radiation in relation to the diameter of the input beam and the power distribution in its cross section.

2. Optical rotatory dispersion in quartz and paratellurite

Currently, the optically active materials most widely applied in laser technology are SiO_2, TeO_2 and $LiIO_3$ (lithium iodate) crystals. The first two materials were used in the depolarisers described below. To provide reliable optical rotatory dispersion data for our calculations, we performed a search for relevant information in the literature and Internet [7–16]. The reason for this was that even modern handbooks on physical quantities provide limited, fragmentary optical rotation data, especially for the IR spectral region. The main results of the literature search are presented in Table 1. For quartz we obtained the following best-fit relation:

$$\rho = a_1 + a_2 \exp\left(-\frac{\lambda}{a_3}\right) + a_4 \exp\left(-\frac{\lambda}{a_5}\right) + a_6 \exp\left(-\frac{\lambda}{a_7}\right), \quad (2)$$

where $a_1 = 1.65569432$, $a_2 = 1104.28722386$, $a_3 = 0.09862624$, $a_4 = 181.71620197$, $a_5 = 0.05857032$, $a_6 = 88.56794745$, $a_7 = 0.35912872$, ρ is in deg mm^{-1} and λ is in microns.

Table 1.

λ/μm	ρ/deg mm^{-1}			
	SiO_2		TeO_2	
	Experiment	Fit	Experiment	Fit
0.408	48.1	47.9	–	368.7
0.4152	–	46.1	337.6	338.5
0.4382	–	40.9	271	272.6
0.463	–	36.2	221	222.7
0.48	33.7	33.5	–	196.7
0.4995	–	30.7	171.2	172.5
0.532	26.7	26.8	143.4	143.4
0.546	25.5	25.4	–	131.2
0.5893	21.7	21.6	104.9	105.5
0.6328	18.7	18.7	86.9	87.1
0.7	–	15.2	67.4	67.3
0.731	13.8	13.9	–	60.4
0.795	11.6	11.7	–	49.4
0.8	–	11.5	48.5	48.7
0.9	–	9	37.4	37.1
1	–	7.2	29.5	29.4
1.064	6.2*	6.3	26.0*	25.9
1.08	–	6.05	–	24.9
1.085	6.1	6	–	24.6
1.1	–	5.8	23.8	23.9
1.142	5.5	5.4	–	22
1.153	5.3	5.2	–	21.6
1.177	5.1	5	–	20.7
1.3	4.2	4	17	16.8
1.55	–	2.8	11.5	11.5
1.565	2.6*	2.8	11.4*	11.5

* This work

For TeO_2 we present an optimised, more accurate relation, obtained from Eqn. (5) in Ref. [14] (that study was concerned with best-fit expressions for the optical rotatory dispersion in paratellurite) by averaging the discrepancies between experimental and theoretical data:

$$\rho = \left[43.2\left(\lambda^2 - 0.08099716\right)^{-1} - 17.7\left(\lambda^2 - 0.04293184\right)^{-1}\right] \times (1.008 - 0.0372\lambda)^{-1}. \quad (3)$$

Table 1 gives also the results of the present ρ measurements at the wavelengths of ytterbium- and erbium-doped superluminescent optical fibre sources ($\lambda_{Yb} = 1.064$ μm, $\lambda_{Er} = 1.565$ μm, spectral width $\Delta\lambda \sim 24$ and 30 nm, respectively).

$LiIO_3$ crystals are very similar in optical activity to TeO_2 crystals, at least in the near-IR. At $\lambda = 0.63$, 1.08, 1.1, 2.0

* Uniaxial crystals, including quartz ($SiO)_2$) and paratellurite (TeO_2), exhibit the highest optical activity along their optical axis [6].

** In contrast to birefringent depolarisers, the wedges of Cornu depolarisers made of uniaxial crystals can readily be brought into optical contact, in particular because such crystals are uniform in thermal expansion across their optical axis.

and 3.7 μm, the ρ of $LiIO_3$ is 80.0, 25.0, 23.8, 7.0 and 2.1 deg mm^{-1}, respectively [17]. These values almost coincide with the ρ values calculated for TeO_2 at the above wavelengths by Eqn (5) in Ref. [14]. Therefore, under permissible service conditions paratellurite crystals can be replaced by large, optically perfect and, nevertheless, relatively cheap lithium iodate crystals.

3. Calculational approach and experimental setup

The calculation procedure corresponded to the following geometry: a collimated plane-polarised beam with an arbitrary polarisation orientation and a Gaussian (diameter $2w_0 = 5$ mm at a $1/e^2$ level) or uniform power distribution passes through interchangeable apertures 2, 3, or 5 mm in diameter and enters the depolariser. The beam was divided into multiple zones, and the angle of optical rotation was computed for each zone. Next, we computed the projections of the electric vectors onto the x and y axes of an analyser placed behind the depolariser and the sums of the corresponding intensities, I_x and I_y, in each zone. The degree of polarisation of the output beam was evaluated from the polarisation extinction ratio

$$\mathrm{Ext} = 10 \lg \frac{\sum I_y}{\sum I_x}. \quad (4)$$

The experimental setup is shown schematically in Fig. 2. The power-stabilised unpolarised output of a superluminescent source made from isotropic ytterbium-doped silica fibre ($\lambda = 1064$ nm, $\Delta\lambda = 24$ nm, output power $P_{\mathrm{out}} = 18$ mW) was collimated, apertured and then polarised by a Thompson prism. A half-wave plate consisting of two quarter-wave Fresnel rhombi rotatable about the beam axis was used to rotate the polarisation plane of the input beam in the range $0-360^\circ$ in order to vary the polarisation state of the light entering the Cornu depolariser. We fabricated four depolarisers from SiO_2 and TeO_2 crystals. Each prism consisted of crystalline wedges identical in chemical composition but opposite in the direction of optical rotation. From either material, we made two depolarisers in the shape of parallelepipeds elongated along their optical axis, of dimensions $10 \times 10 \times 22.3$ (SiO_2) and $10 \times 10 \times 20.7$ mm (TeO_2) along the x, y and z axes, respectively (Fig. 1). The wedges were bonded by optical contacting. The polarisation extinction ratio integrated over the cross section of the output beam was analysed using two Anritsu ML9001A precision power meters, which had a dynamic range over 10^6.

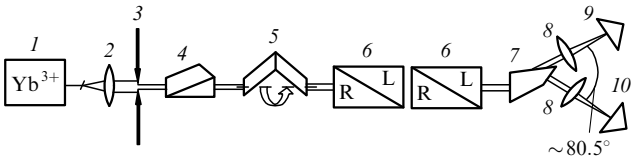

Figure 2. Experimental setup for investigation of Cornu depolarisers: (*1*) stabilised superluminescent source, (*2*) lens collimator, (*3*) interchangeable apertures, (*4*) Thompson polariser, (*5*) half-wave plate consisting of two Fresnel rhombi, (*6*) two depolarisers to be studied, (*7*) calcite prism/analyser, (*8*) lenses for focusing the beams onto the active area of power meters, (*9*, *10*) Anritsu ML9001A power meters for p- and s-polarised beams, respectively.

Polarisation splitting of the beams by $\sim 80^\circ$ was achieved using a calcite prism polarisation splitter with minimised reflection losses for all light beams [18]. The prism had a shape, utilised for the first time, such that the p-polarised extraordinary wave left the crystal at Brewster's angle, whereas the unpolarised incident and ordinary waves propagated normal to the bloomed faces of the prism.

4. Results

Figures 3–8 present our measurement and calculation results on the polarisation extinction in the Cornu depolarisers. The curves in Fig. 3 illustrate the depolarising power of the quartz device as a function of the polarisation orientation of a Gaussian input beam for two apertures and two depolariser lengths (the length was doubled by placing two samples in series, as shown in Fig. 2). In Fig. 3, zero angle corresponds to the polarisation plane oriented vertically; the transmission axes of the analysers were oriented vertically and horizontally, and the depolarisers were mounted so that the diagonal interfaces between the crystals were vertical. Dashed curve (*2*) represents the calculation results for a single depolariser of length $L = 22.3$ mm, with the reference value of the optical rotatory power of quartz, $\rho(1064\ \mathrm{nm}) = 6.2$ deg mm^{-1}, and an aperture diameter $d = 2$ mm. As seen, there is good agreement with measured curve (*1*). Clearly, lower extinction values, e.g. Ext $\leqslant 1$ dB, can only be achieved with $L \geqslant 44.6$ mm and $d \geqslant 5$ mm [curve (*5*)].

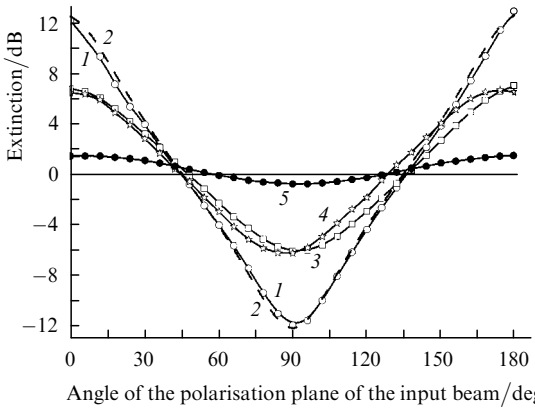

Figure 3. (*1*, *3*–*5*) Measured and (*2*) calculated polarisation extinction ratio as a function of the polarisation orientation of the input beam ($\lambda = 1064$ nm) for Cornu depolarisers made from optically active SiO_2 crystals: (*1*–*3*) one depolariser, $L = 22.3$ mm; (*4*, *5*) two depolarisers, $L = 44.6$ nm; aperture diameter of (*1*, *2*, *4*) 2 and (*3*, *5*) 5 mm.

Notably better results (Fig. 4) were obtained with the depolarisers made from TeO_2 crystals, which offer much higher optical activity: $\rho(1064\ \mathrm{nm}) = 26$ deg mm^{-1}. However, the calculation results for these depolarisers differ considerably from the experimental data, in contrast to the quartz depolarisers. For example, the y intercept of measured curve (*1*) was Ext ~ 2.2 dB, whereas the calculated value was Ext $= 0.45$ dB. Good agreement between curves (*1*) and (*2*) was only achieved with a lower optical rotatory power, $\rho(1064\ \mathrm{nm}) = 21$ deg mm^{-1}. Therefore, the performance of the depolariser was equivalent to that of a less optically active material. We tentatively attribute this

inconsistency to both the errors in the mutual orientation of the crystalline samples and the possible optical inhomogeneity of the bulk TeO_2 crystals opposite in the direction of rotation. The former assumption is based on the fact that, in uniaxial crystals with a sufficiently large birefringence, $|n_e - n_o| \geqslant 0.01$, the optical rotatory power drops sharply just a few degrees off the optical axis of the crystal [6]. TeO_2 has a high birefringence, $n_e - n_o \approx 0.14$, which by far satisfies the above inequality. Therefore, in fabricating TeO_2 prisms for a depolariser special attention should be paid to crystallographic orientation accuracy and the optical quality of the crystals. In this regard, large, more optically perfect $LiIO_3$ crystals grown from solution have a significant advantage over melt-grown TeO_2 crystals.

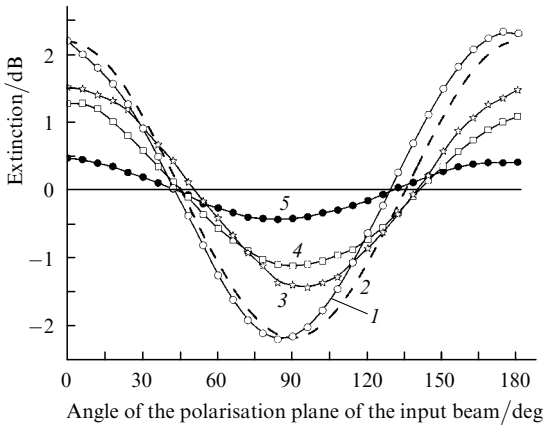

Figure 4. (*1*, *3*–*5*) Measured and (*2*) calculated polarisation extinction ratio as a function of the polarisation orientation of the input beam for Cornu depolarisers made from optically active TeO_2 crystals: (*1*–*3*) one depolariser, $L = 20.7$ mm; (*4*, *5*) two depolarisers, $L = 41.4$ nm; aperture diameter of (*1*, *2*, *4*) 2 and (*3*, *5*) 5 mm.

It is worth noting that, in Figs 3 and 4, the extinction ratio has maxima at 0, 90°, 180°, 270° and 360°. This was taken into account in further calculations, which were all made for zero angle.

Figures 5–8 show the calculated extinction ratio as a function of rotatory power (material and wavelength), depolariser length L and aperture diameter for Gaussian and uniform beams. The diameter of the Gaussian beam was taken to be constant ($2w_0 = 5$ mm), whereas that of the uniform beam was determined by the aperture. An interesting feature of the data in Figs 5–8 is that the curves intersect the abscissa ($I_x = I_y$) in a systematic manner. This suggests that, rather than choosing crystals with as high an optical activity as possible, one can take advantage of a material with an optical activity corresponding to the first zero of extinction (Fig. 5). To this end, however, the depolariser length L and aperture diameter must be properly adjusted to the particular beam profile.

It follows from Figs 5–8 that, under comparable conditions, low extinction values are easier to achieve for uniform beams than for Gaussian ones. The reason for this is that the periphery of a Gaussian beam contributes less to the polarisation state of the output beam than does the periphery of a uniform beam. Moreover, the intermixing of polarisation states is more effective when the power distribution is broader (for an infinitely narrow beam, no depolarisation occurs). Therefore, one must use as broad

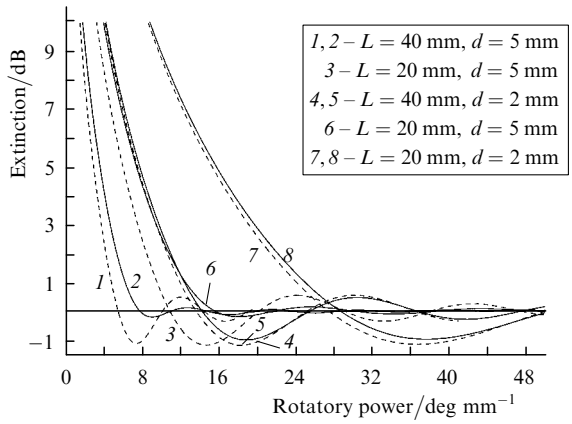

Figure 5. Calculated polarisation extinction in Cornu depolarisers as a function of optical rotatory power for Gaussian ($2w_0 = 5$ mm, solid lines) and uniform (dashed lines) beams.

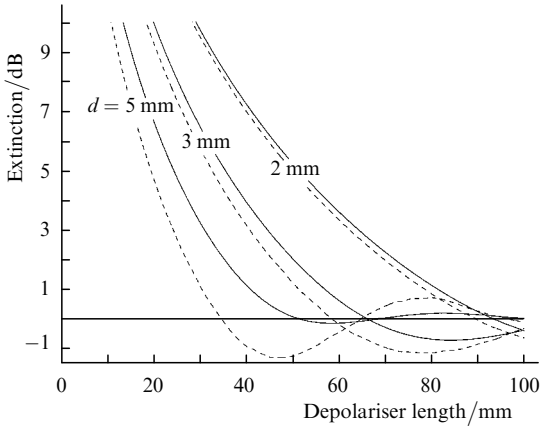

Figure 6. Calculated polarisation extinction in quartz Cornu depolarisers as a function of depolariser length for Gaussian (solid lines) and uniform (dashed lines) beams; $\lambda = 1.064$ μm.

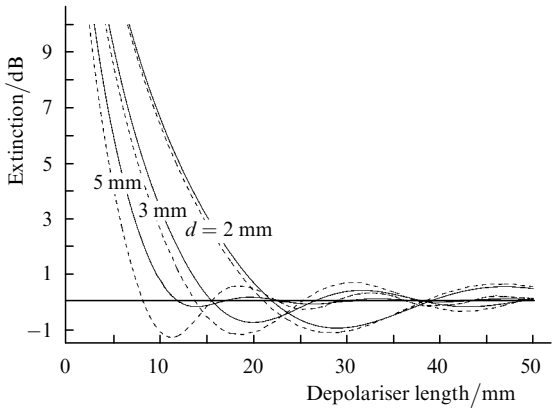

Figure 7. Calculated polarisation extinction in paratellurite Cornu depolarisers as a function of depolariser length for Gaussian (solid lines) and uniform (dashed lines) beams; $\lambda = 1.064$ μm.

beams as possible. The choice of the depolariser length L depends on the ability to grow large, high-quality crystals with both directions of optical rotation. Unfortunately, manufactures typically provide only one enantiomorph. This problem can be alleviated to some extent by placing several short depolarisers in series, as shown in Fig. 2. It is even possible to get by with crystals of the same enantio-

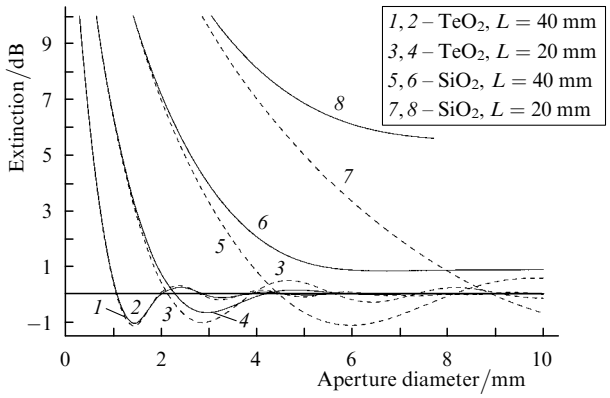

Figure 8. Calculated polarisation extinction in Cornu depolarisers as a function of input aperture diameter for Gaussian (solid lines) and uniform (dashed lines) beams; $\lambda = 1.064$ μm.

morph, using a compensating glass wedge instead of the second crystal (drawback of large L).

In choosing the design and material of Cornu depolarisers, one must take into account that the circularly polarised output beams are non-parallel. The angle between the almost symmetrically deflected beams in air is given by (Fig. 1)

$$\Delta\theta = \arcsin[n_R \sin(\alpha - \beta_1)] - \arcsin[n_L \sin(\alpha - \beta_2)], \quad (5)$$

where

$$\alpha = \arctan(L/H); \quad \beta_1 = \arcsin[(n_L/n_R)\sin\alpha];$$

$$\beta_2 = \arcsin[(n_R/n_L)\sin\alpha].$$

Figure 9 shows the calculated angle between the output beams as a function of wavelength for SiO_2 ($L = 44.6$ mm, $H = 10$ mm) and TeO_2 ($L = 41.4$ mm, $H = 10$ mm) Cornu depolarisers. Also presented for comparison are the calculation results for birefringent depolarisers consisting of a quartz wedge and BK-8 glass wedge with wedge angles of 10° and 20°. In those calculations, we used the ρ values given in Table 1, the Sellmeyer formulas for the refractive indices of quartz [19], standard dispersion formulas for glass [20] and best-fit equations for the $n_o(\lambda)$ and $n_e(\lambda)$ of paratellurite, which had been derived from reference refractive index data [21]:

$$n_o(SiO_2) = \left(3.53445 + \frac{0.008067}{\lambda^2 - 0.0127493} + \frac{0.002682}{\lambda^2 - 0.000974} + \frac{127.2}{\lambda^2 - 108}\right)^{1/2}, \quad (6)$$

$$n_e(SiO_2) = \left(3.5612557 + \frac{0.00844614}{\lambda^2 - 0.0127493} + \frac{0.00276113}{\lambda^2 - 0.000974} + \frac{127.2}{\lambda^2 - 108}\right)^{1/2}, \quad (7)$$

$$n_{o,e}(TeO_2) = b_1 + b_2 \exp\left(-\frac{\lambda}{b_3}\right) + b_4 \exp\left(-\frac{\lambda}{b_5}\right) + b_6 \exp\left(-\frac{\lambda}{b_7}\right), \quad (8)$$

where λ is in microns;

$$b_1 = 2.18684117, \quad b_2 = 0.58914524, \quad b_3 = 0.27786593,$$

$$b_4 = 3.51109821, \quad b_5 = 0.10582791, \quad b_6 = 0.49931817,$$

$$b_7 = 0.11062601$$

for the ordinary wave and

$$b_1 = 2.3327039, \quad b_2 = 1.08795949, \quad b_3 = 0.1328851,$$

$$b_4 = 0.67839706, \quad b_5 = 0.21415973, \quad b_6 = 0.67353531,$$

$$b_7 = 0.20848677$$

for the extraordinary wave.

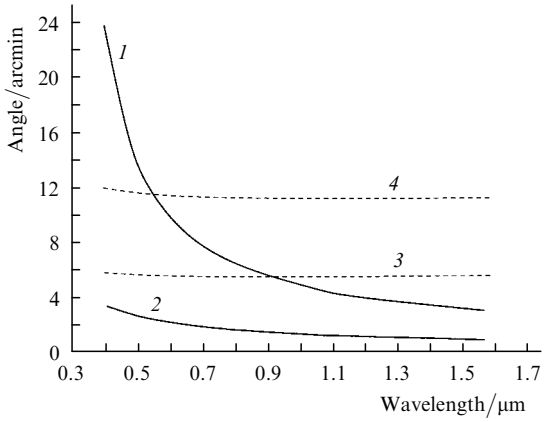

Figure 9. Calculated angle between the output beams as a function of wavelength for (*1*) TeO_2 ($H = 10$ mm, $L = 41.4$ mm) and (*2*) SiO_2 ($H = 10$ mm, $L = 44.6$ mm) Cornu depolarisers and for (*3*, *4*) birefringent depolarisers consisting of a quartz crystal wedge and BK-8 glass wedge with wedge angles of 10° and 20°, respectively.

As expected, in the near-IR the angle between the circularly polarised output beams is substantially smaller than that at the output of birefringent depolarisers, in spite of the large wedge angle in the Cornu depolariser. The use of paratellurite Cornu depolarisers in the visible range may seem questionable. This is however not so because in this range the rotatory power rises quadratically with frequency [6] and, hence, a smaller depolariser length is needed; so the angle between the output beams will be smaller. Our calculations indicate that, for Cornu depolarisers, this angle is an almost linear function of L ($H = \text{const}$), in contrast to that for birefringent depolarisers, which slightly deviates from linearity, but not very much, at least for wedge angles below 45°. To verify the calculation results, we measured the angle between Gaussian beams from an He–Ne laser ($\lambda = 0.6328$ μm, collimated beam 3 mm in diameter, 35-m spacing, ~ 10 % measurement accuracy) at the output of a Cornu depolariser consisting of two rectangular quartz prisms placed as shown in Fig. 2. The measured angle, $2'$, is

in perfect agreement with the value obtained by Eqn (5), namely, $2.02'$. Using a thin film polariser, we found that both beams were circularly polarised.

5. Conclusions

We investigated two Cornu depolarisers made from materials differing markedly in optical rotatory power. Experimental data and numerical calculations demonstrate that this type of depolariser makes it possible to significantly alleviate the drawback common to birefringent wedge depolarisers: 100 % dependence of the polarisation of the output beam on the input polarisation orientation.

In calculations of the depolariser design, one must take into account not only properties of the material but also the desired aperture size and the power distribution across the input beam.

In preparing optically active crystals for cutting, particular attention should be paid to the maximum possible accuracy in their orientation relative to the optical axis (uniaxial crystals) or the crystallographic axis of the highest optical activity (biaxial crystals and optically isotropic crystals with cubic symmetry). According to our estimates, the orientation must be accurate to within $\pm 15'$.

References

1. Billings B.H. *J. Opt. Soc. Am. C*, **41**, 966 (1951).
2. Mochizuki K. *Appl. Opt*., **23** (19), 3286 (1984).
3. McGuire J.P., Chipman R.A. *Opt. Eng*., **29** (12), 1478 (1990).
4. http://www.novaphase.com; http://www.klccgo.com; http://www.cvilaser.com.
5. Davydov B.L., Voshinsky E.A., Voshinsky Yu.A. *Proc. 3rd Int. Symp. on High-Power Fiber Lasers and their Application* (St. Petersburg, Russia, 2006, HPFL–P1) p. 5.
6. Sirotin Yu.I., Shaskol'skaya M.P. *Osnovy kristallofiziki* (Fundamentals of Crystal Physics) (Moscow: Nauka, 1975).
7. Mindlin R.D., Toupin R.A. *Proc. 25th Annual Symp. on Frequency Control* (Atlantic City, NJ, 1971) p. 58.
8. http://www.minsocam.org/ammin/AM37/AM37.158.pdf.
9. Chou C., Huang Y.C., Chang M. *Appl. Opt*., **36** (16), 3604 (1997).
10. Ward R.W. *Proc. 14th Piezoelectric Devices Conf. and Exhibition* (Salt Lake City, 1992).
11. http://www.kayelaby.npl.co.uk./general.physics/2.5/2.5.10.html; http://www.impex-hightech.de.
12. Uchida N. *Phys. Rev. B*, **4** (10), 3736 (1971).
13. Jankm V., Vysin V. *Opt. Commun*., **3** (5), 308 (1971).
14. Belyaev et al. *Kristallografiya*, **20** (6), 1221 (1975).
15. Kaminsky W., Glazer A.M. *Ferroelectrics*, **183**, 133 (1996).
16. Kaminsky W. *Rep. Progr. Phys*., **63**, 1575 (2000).
17. http://www.clevelandcrystals.com/LiIO3.htm.
18. Davydov B.L. *Kvantovaya Elektron*., **36** (5), 473 (2006) [*Quantum Electron*., **36** (5), 473 (2006)].
19. http://www.ieee-uffc.org/freqcontrol/quartz/fc.conqtz2.html.
20. Dolgova L.N. (Ed.) *Bestsvetnoe opticheskoe steklo SSSR* (katalog) (Colourless Optical Glass in the USSR: A Catalogue) (Moscow: Dom Optiki, 1990).
21. http://www.sciner.com/Crystals/TeO2.htm; http://www.almazoptics.com/TeO2.htm.